Electronic Supplementary Material (ESI) for Nanoscale Horizons.

Supporting Information

Size-Tunable Rhodium Nanostructures for Wavelength-Tunable Ultraviolet Plasmonics

Xiao Zhang,[1] Pan Li,[1] Ángela Barreda,[2] Yael Gutiérrez,[2] Francisco González,[2] Fernando Moreno,[2] Henry O. Everitt,[3,4,*] and Jie Liu[1,*]

[1]*Department of Chemistry, Duke University, Durham, NC 27708*

[2]*Optics Group, Department of Applied Physics, University of Cantabria, Avda de Los Castros, s/n 39005 Santander, Spain*

[3]*Department of Physics, Duke University, Durham, NC 27708*

[4]*C.M. Bowden Laboratory, Army Aviation & Missile RD&E Center, Redstone Arsenal, AL 35898*

Email: j.liu@duke.edu, everitt@phy.duke.edu

Experimental section

Seedless synthesis of Rh nanocubes (NCs)

0.45 mmol potassium bromide (KBr, Acros) and 2 mL ethylene glycol (EG, J. T. Baker) were added to a 20 mL vial (cleaned with detergent and deionized water, and dried in a vacuum oven at 80 ^{o}C) equipped with a Teflon-coated magnetic stir bar. The colorless solution was heated in an oil bath held at 160 ^{o}C for 40 min with loosely placed cap. Meanwhile, 0.045 mmol rhodium(III) chloride hydrate ($RhCl_3 \cdot xH_2O$, 38% Rh, Acros) and 0.225 mmol polyvinylpyrrolidone (PVP, in terms of repeating unit, M.W. ≈ 55,000, Aldrich) were separately dissolved in 2 mL EG at room temperature. These two solutions were injected simultaneously into the vial by a two-channel syringe pump at a rate of 1 mL/h. After injection, the reaction mixture was held at 160 ^{o}C for another 10 min and then cooled to room temperature. 27 nm Rh NCs were obtained with this amount of Rh precursor and smaller NCs could be synthesized by reducing the amount of precursor.

Seed-mediated synthesis of Rh NCs

0.4 mL of the reaction mixture of 27 nm Rh NCs was diluted with 1.6 mL EG in a cleaned 20 mL vial with stirring. The reaction mixture was heated in an oil bath held at 160 ^{o}C for 40 min with loosely placed cap. 0.045 mmol $RhCl_3 \cdot xH_2O$ was dissolved in 2 mL EG, and 0.225 mmol PVP and 0.45 mmol KBr were co-dissolved in another 2 mL EG. These two solutions were injected into the vial simultaneously by syringe pump at a rate of 1 mL/h. The reaction mixture was held at the reaction temperature for another 10 min and then cooled to room temperature. 59 nm Rh NCs were synthesized with this amount of Rh precursor and NCs with edge lengths between 27 and 59 nm could be obtained by reducing the amount of precursor. These Rh NCs

were collected by centrifugation, washed with water/acetone for several times and dispersed in ~5 mL ethanol, respectively, for further characterization.

Sample preparation for Raman measurements

Si wafers were cut into ~4×4 mm substrates. 10 μL of 21, 39, and 59 nm Rh NCs dispersed in ethanol were drop-coated on the Si substrates and dried in ambient condition, respectively. These substrates were rinsed with ethanol and dried by air to leave a submonolayer of Rh NCs, which were subsequently immersed in 5 mM *p*-aminothiophenol (PATP) in ethanol solution for 24 h (covered). After that, these samples were rinsed with ethanol to remove excess PATP not attached to the Rh NCs. For the neat PATP sample, a Si substrate was dip-coated by 5 mM PATP solution and dried in ambient condition. AFM measured the thickness to vary between 50-100 nm.

Material Characterization

Scanning electron microscopy (SEM) images were obtained by using an FEI XL30 FEGSEM. Transmission electron microscopy (TEM) and high-resolution TEM (HRTEM) images were collected by a FEI Tecnai G^2 Twin operating at 200 kV. UV-vis extinction spectra were obtained by a Shimadzu UV-3600. Raman spectroscopy was carried out on a Horiba Jobin Yvon LabRam ARAMIS. Atomic force microscopy (AFM) images were collected by a Digital Instruments Dimension 3100 operating in tapping mode.

Theoretical Simulation

The interaction of electromagnetic radiation with Rh NCs has been investigated through the finite element method implemented in the commercial software COMSOL Multiphysics 4.4.[1] In

particular, we used the RF Module, which allows us to formulate and solve the differential form of Maxwell's equations in the frequency domain together with the initial and boundary conditions. The equations are solved using the finite element method with numerically stable edge element discretization in combination with state-of-the-art algorithms for preconditioning and solving the resulting sparse equation systems.

The simulated Rh NCs were immersed in an ethanol sphere whose radius corresponded with the wavelength of the incident radiation. A perfectly matched layer (PML) domain is placed outside of the embedding medium domain to act as an absorber of the scattered field. The mesh was fine enough as to allow convergence of results. The spectral extinction cross-section C_{ext} is calculated as the sum of the corresponding absorption C_{abs} and scattering C_{sca} cross-sections,

$$C_{ext} = C_{abs} + C_{sca} \quad . \tag{1}$$

C_{abs} can be calculated as the integral of resistive losses over the NC's volume (l^3 for a cube of size l), normalized to the incident power density, S, defined as

$$S = \frac{|E(r)|}{2\,Z_{sm}} \quad , \tag{2}$$

where $\boldsymbol{E}(r)$ is the local electric field. Z_{sm} is the impedance of the surrounding medium

$$Z_{sm} = \frac{Z_0}{n_{sm}} = \frac{\mu_0 c}{n_{sm}} \quad , \tag{3}$$

where μ_0 and c are the permeability and light speed in vacuum, respectively, and n_{sm} refers to the refractive index of the surrounding medium.

The scattering cross-section C_{sca} is derived by integrating the Poynting vector over an imaginary sphere around the NC, normalized again to the incident power density S. The absorption and scattering efficiencies, Q_{abs} and Q_{sca} respectively, are defined through the equations

$$Q_{abs} = \frac{C_{abs}}{A}, \qquad Q_{sca} = \frac{C_{sca}}{A}, \tag{4}$$

where A is the NC cross-sectional area projected onto a plane perpendicular to the incident beam (e.g., $A=l^2$).

The real and imaginary parts of the dielectric function ε for Rh were respectively calculated from the following analytical expressions,

$$Re(\varepsilon) = 0.17 + \frac{-100 - 0.17}{1 + \left(\frac{600\,\pi\,0.54}{\lambda}\right)^2} \tag{5}$$

$$Im(\varepsilon) = \frac{(-100 - 0.17)\left(\frac{600\,\pi\,0.54}{\lambda}\right)}{1 + \left(\frac{600\,\pi\,0.54}{\lambda}\right)} + \frac{1.7e^6}{\frac{600\,\pi\,8.85e^3}{\lambda}}.$$

These equations were obtained by fitting the tabulated values[2] to a Debye-Drude model. The refractive index of ethanol was considered to be 1.4. The structure was illuminated, under normal incidence by a plane wave polarized along the x-axis and propagating along the z-axis, as shown in Fig. 4.

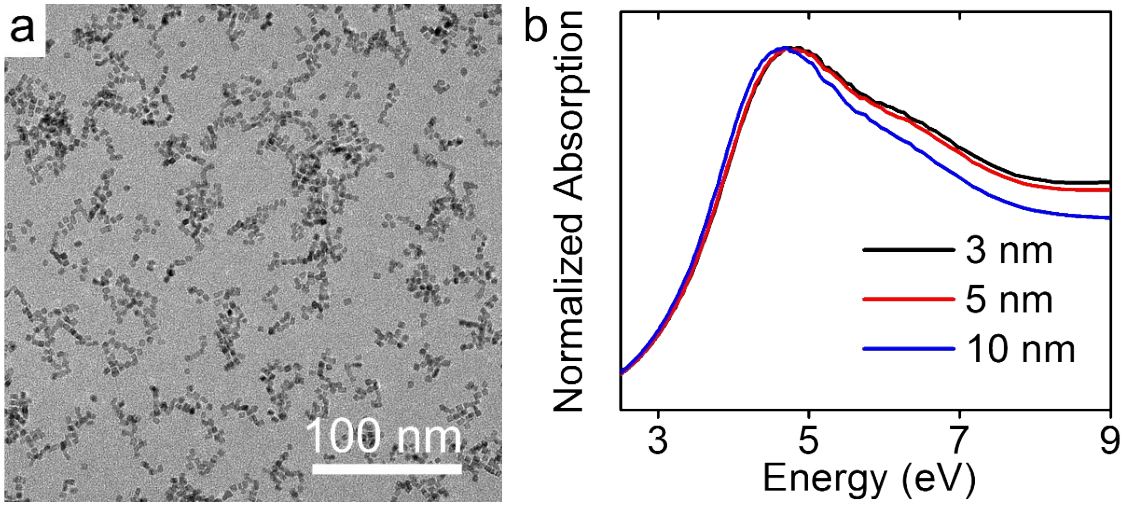

Fig. S1. Representative TEM image of Rh NCs with edge length of 3 nm (a) and simulated absorption spectra of small Rh NCs in ethanol (b). The local surface plasmon resonance (LSPR) energies of dipolar modes of Rh NCs smaller 10 nm are higher than 4.8 eV, above the detection range of our spectrometer.

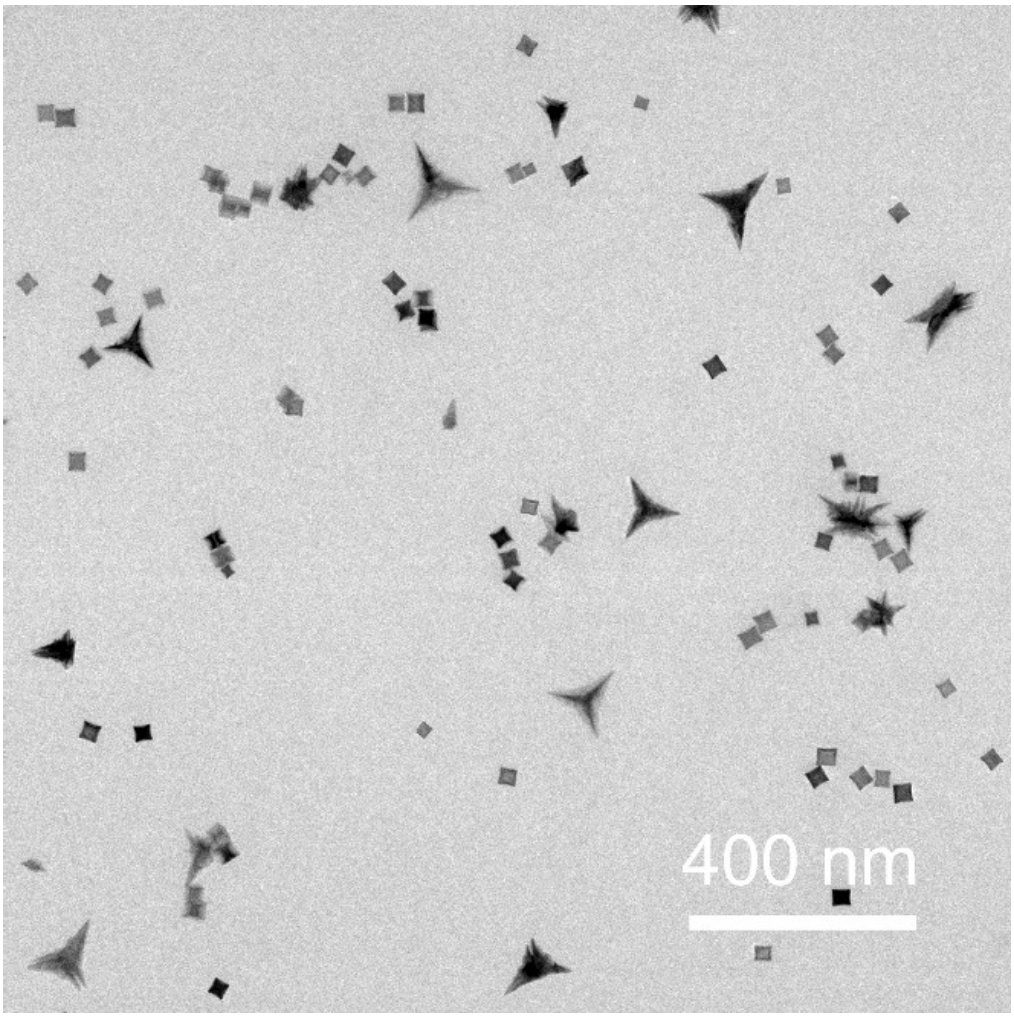

Fig. S2. TEM image of Rh nanoparticles synthesized from seedless slow-injection method with an injection time of 3 h. Other than Rh NCs, tripods and irregular nanoparticles were observed, indicating the failure of shape control with prolonged injection time.

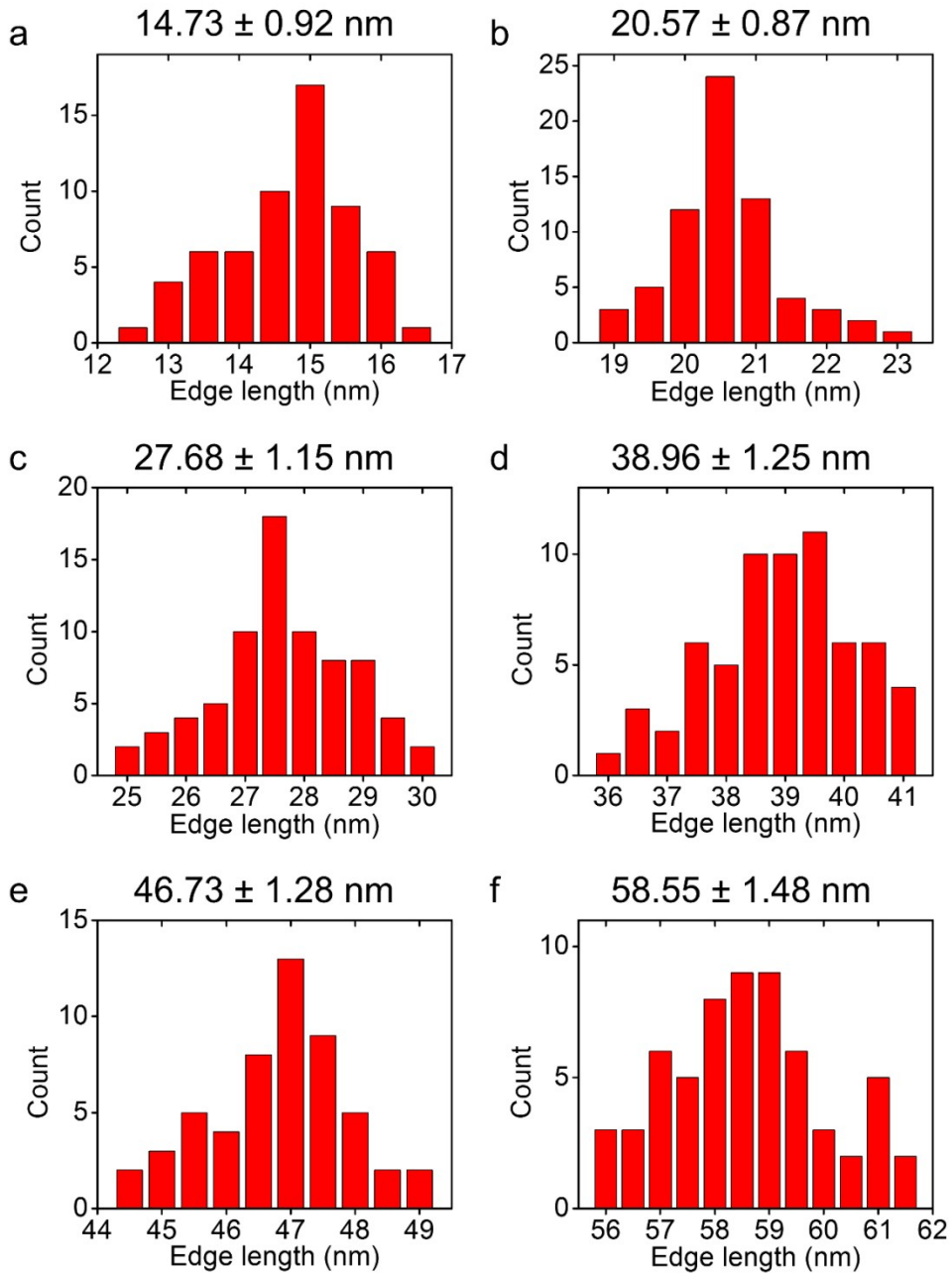

Fig. S3. Edge length distribution and standard deviation (SD) of Rh NCs with edge length of 15 (a), 21 (b), 27 (c), 39 (d), 47 (d) and 59 nm (e), respectively. The narrow size distribution (SD < 1.5 nm) shows the size uniformity of the Rh NCs synthesized by seedless and seed-mediated slow-injection methods.

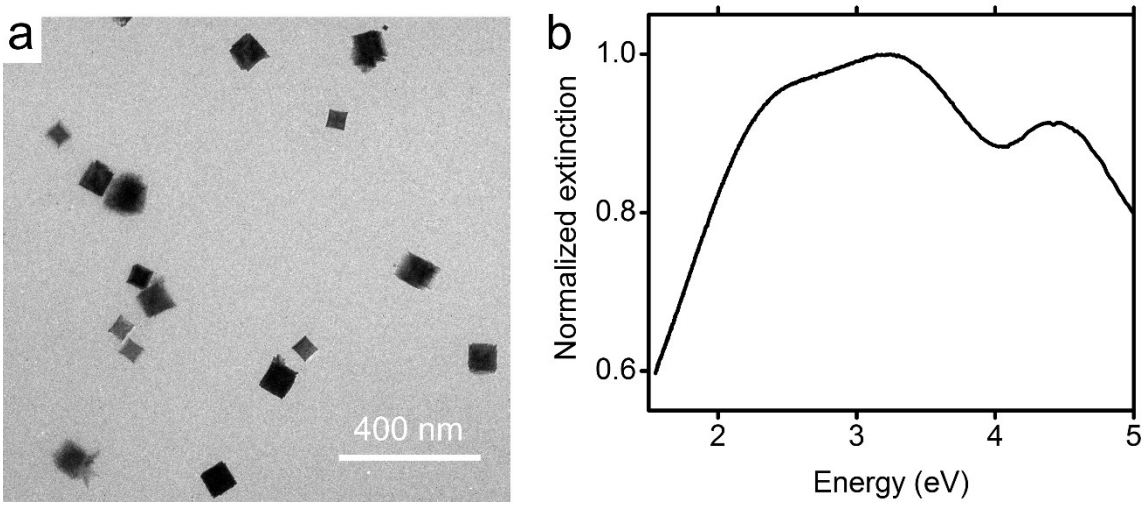

Fig. S4. Representative TEM image (a) of Rh NC sample containing NCs with edge lengths larger than 90 nm and corresponding UV-vis extinction spectrum (b). The LSPR energies can be extended into the visible region (~2.3 eV). The broad LSPR can be attributed to the non-uniform sizes of the Rh NCs.

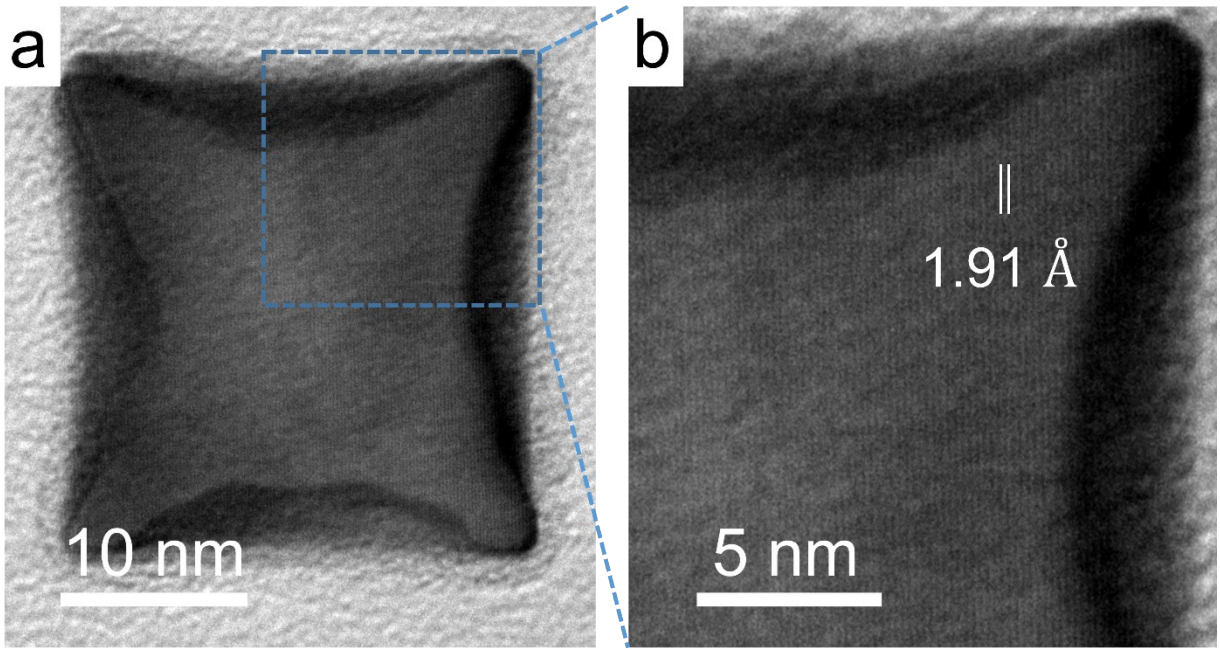

Fig. S5. HRTEM image of a 26.0 nm Rh NC recorded along the [100] zone axis (a) and the zoom-in image of its corner (b). The 1.91 Å lattice spacing, parallel to the faces of Rh NC, corresponds to the {200} planes of face-centered cubic Rh crystal, indicating that the Rh NCs are mainly encapsulated by {100} facets. The contrast along the edge shows the concave nature of the faces.

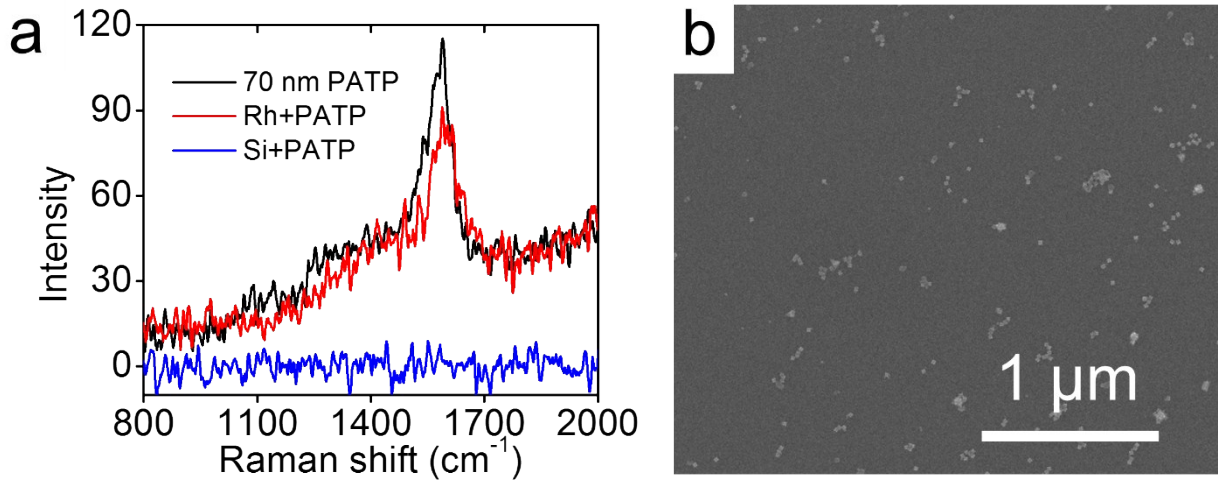

Fig. S6. a, Raman spectra of the 70 nm PATP layer (black), PATP monolayer on 39 nm Rh NCs (red) and Si substrate following the same PATP coating procedure but without Rh NCs (Si+PATP, blue). The weak signal, which is barely noticeable within the instrument noise, of the Si+PATP sample supports that the enhancement of Raman signal indeed comes from the excitation of LSPR in Rh NCs. b, SEM image of 39 nm Rh NCs deposited on the surface of Si substrate. The Rh NCs together covered ~3% of the underlying substrate.

Supplementary references

1. COMSOL Multiphysics 4.4, http://www.comsol.com, (accessed May 5, 2015).
2. E. Palik and J. M. Bennett, *Handbook of Optical Constants of Solids I and II*, Academic Press, New York, 1995.